

LCLS Gun Solenoid Design Considerations*

John Schmerge

Abstract

The LCLS photocathode rf gun requires a solenoid immediately downstream for proper emittance compensation. Such a gun and solenoid have been operational at the SSRL Gun Test Facility (GTF) for over eight years. Based on magnetic measurements and operational experience with the GTF gun solenoid multiple modifications are suggested for the LCLS gun solenoid. The modifications include adding dipole and quadrupole correctors inside the solenoid, increasing the bore to accommodate the correctors, decreasing the mirror plate thickness to allow the solenoid to move closer to the cathode, cutouts in the mirror plate to allow greater optical clearance with grazing incidence cathode illumination, utilizing pancake coil mirror images to compensate the first and second integrals of the transverse fields and incorporating a bipolar power supply to allow for proper magnet standardization and quick polarity changes. This paper describes all these modifications plus the magnetic measurements and operational experience leading to the suggested modifications.

I. INTRODUCTION

a. Need for a solenoid

The LCLS gun solenoid is used to focus the beam immediately downstream of the cathode. The beam experiences strong rf and space charge defocusing forces and a lens is required to contain the beam. The rf defocusing kick at the gun exit acts like a lens [1] with a calculated focal length of -10 cm for a 6 MeV beam energy and a 120 MV/m on axis field in the gun as desired in the LCLS injector.

In addition the space charge force defocuses the electron beam. An externally applied lens is required to focus the beam downstream of the gun for the so called "emittance compensation" [2]. Emittance compensation is a technique to reduce the transverse, projected emittance of both the x and y planes. Without emittance compensation, the phase space of each temporal slice of the transverse emittance evolves differently due to the different space charge and rf forces experienced by each slice leading to a projected emittance growth. With emittance compensation, the phase space ellipse of each slice is brought back into alignment downstream of the gun with a focusing element and the emittance finally frozen by additional acceleration. Optimum compensation occurs when all temporal phase space ellipses align to produce the minimum projected emittance.

Since the external magnetic focusing element is linear (linear kick vs transverse distance from the center), the rf and space charge forces must also be linear for optimal

* Work supported in part by the DOE Contract DE-AC02-76SF00515.
This work was performed in support of the LCLS project at SLAC

ellipse alignment. The rf term is linear for small beam sizes and the space charge force is approximately linear for a temporally flat electron beam distribution with a round, uniform density cross section. This is the so called temporal and spatial flat-top distribution desired in the LCLS injector. A true linear space charge force is obtained with the so called water bag distribution [3] but is more difficult to create with the laser. Since the rf and space charge forces are radially symmetric, (neglecting aberrations and assuming a round beam at the cathode) the focusing force must also be radially symmetric or by symmetry the beam will not be optimally compensated in both planes. Therefore a solenoid lens is required instead of a quadrupole doublet or triplet and the compensation occurs simultaneously in both the x and y planes.

The applied focusing will ideally start immediately downstream of the cathode since any beam created inside a solenoid field will end up with non-zero angular momentum downstream in the field free region according to Busch's Theorem [4]. If the solenoid field is not zero at the cathode a bucking coil behind the cathode may be required to reduce the total solenoid field to acceptable levels. If the focusing is applied too far downstream the compensation may not be optimum because the beam size can become too large and experience non-linear rf defocusing. Thus there is an optimum position for the lens. To be more precise there is an optimum position for the start of the lens. The lens length is a free parameter provided it is not so long that the beam size grows too large in the gun where the rf defocusing is large. In practice the lens should be as short as practical to allow for diagnostics and other components in the beam-line.

b. Specifications

The basic solenoid specifications are listed in table 1. Despite the calculated rf focal length of -10 cm, the typical optimal solenoid focal length experimentally determined by minimizing the beam emittance at the GTF is typically 16 cm. The solenoid is designed to produce 30% higher field than required. At a maximum beam energy of 7 MeV this corresponds to a 12 cm minimum focal length. The dipole field must be kept to less than a 5 mrad kick and the quadrupole field to greater than 20 m focal length assuming 5 MeV beam energy (approximately the minimum beam energy expected from the LCLS gun). In addition dipole and quadrupole correctors will be included (described later) to cancel any remaining transverse fields. It is also desired that the solenoid field vary linearly with current and the field must be radially symmetric and also axially symmetric to within a few % about the center of the magnet.

The rising edge (edge defined as the 50% of the maximum field point) of the solenoid must be within 11 cm of the cathode to minimize the emittance [5]. It is desired to keep the rising and falling edge width (10%-90% length) to less than 7 cm with a bore greater than 7 cm so the solenoid can slide over a 2.75" conflat flange. The normalized emittance due to a solenoid field at the cathode from Busch's Theorem is given in equation 1 where B_0 is the solenoid field at the cathode and r_0 is the beam radius at the cathode assuming a uniform electron distribution [6]. In order to keep the normalized emittance less than $0.3 \mu\text{m}$ with the LCLS electron beam diameter of 2.4 mm at the cathode requires the cathode solenoid field to be $< 30 \text{ G}$. If this condition is not met, a bucking coil must be added to reduce the field at the cathode over the full diameter of the electron beam. The solenoid axial position must be correct to approximately 1 mm and

the total length of the solenoid should be less than or equal to the prototype solenoid length of 22.5 cm in order to allow as much space as possible for electron beam diagnostics between the rf gun and first linac section.

$$\varepsilon_n = \frac{eB_z r_0^2}{8mc} \quad 1$$

The transverse alignment should be correct to roughly 50 microns or about 5% of the beam size. The pitch and yaw can be corrected by the x,y dipole corrector since the main effect is to steer the beam. Thus the pitch and yaw alignment are approximately 5 mrad. In practice the solenoid is iteratively aligned to the gun by adjusting the solenoid position and then checking the alignment with a beam based technique. Of course the alignment must only be completed once although the beam based alignment verification can be (and in practice is) repeated frequently to verify the alignment has not changed. Since the electron beam is assumed axially symmetric, the roll is considered irrelevant and no specification is given.

Table 1: Gun Solenoid Specifications

Parameter	Value	Conditions
Focal length	12 cm	At 7 MeV
Dipole kick	< 5 mrad	At 5 MeV
Quadrupole focal length	> 30 m	At 5 MeV
Axial Field	< 30 G	At cathode
Maximum Axial Field	4 kG	With 19.5 cm effective length
Maximum Current	275 A	
Cathode to Solenoid Edge	< 11 cm	Edge defined as 50% of maximum
Edge width	< 7 cm	10% to 90% field width
Solenoid Bore	> 7 cm	Must fit over 2.75" flange
Length	< 22.5 cm	
Z position alignment	<1 mm	
X or Y, position alignment	<50 microns	5% of 2 mm beam size
Pitch and Yaw	< 5 mrad	

II. EXPERIMENTAL EXPERIENCE AT GTF

a. Asymmetric electron beam

One of the problems encountered after the first beam was generated at the GTF was the very non uniform electron beam that was evident on phosphor screens immediately downstream of the solenoid. Initially the problem was attributed to a non-uniform laser beam and cathode quantum efficiency. However, after these problems were corrected the electron beam was still not round as measured on the screen despite using a round, flat laser profile to generate the electrons. The beam exhibits very asymmetric features when the beam is nearly focused by the solenoid on the screen. In an attempt to determine the source of the asymmetry the polarity of the solenoid was reversed and the effect on the beam observed. Figure 1 shows an image of the beam approximately 40 cm downstream

of the solenoid exit with both solenoid polarities. The same laser beam profile, beam charge and gun parameters were used to generate the beam. The only parameters changed were the polarity of the solenoid field and small changes to the steering magnets downstream of the solenoid. If the solenoid produced a pure solenoid field the images in figure 1 should just be rotated versions of each other. From the images in figure 1 it is clear the solenoid contains additional fields that have a significant effect on the electron beam.

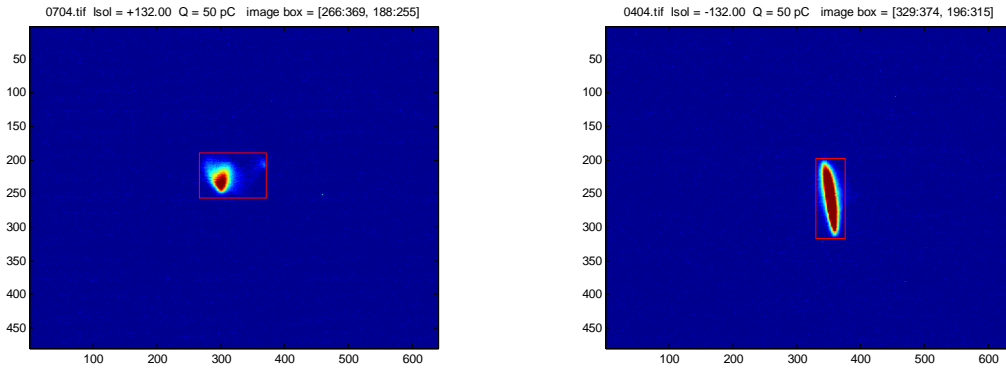


Figure 1: The electron beam image with normal and reversed solenoid polarity.

b. Effective Quadrupole Focal Length

A beam study was conducted to determine the effective quadrupole focal length that would explain the asymmetric beam sizes generated at the GTF. The measured horizontal and vertical beam size vs solenoid field is shown in figure 2. It is clear that the horizontal beam size reaches a minimum at a lower solenoid field than the vertical beam size and the minimum of the vertical beam size is smaller than the minimum horizontal beam size. The figure also includes the calculated beam size assuming identical horizontal and vertical phase space distributions upstream of the solenoid. One of the fit parameters is the focal length of a thin lens located immediately upstream of the solenoid. In order to explain the difference in horizontal and vertical beam sizes requires a lens with approximately a 4m focal length at a beam energy of roughly 5.5 MeV. This lens could be produced by either the rf gun or the solenoid. Based on these observations it was determined that the solenoid should be removed and carefully measured to determine the quadrupole contribution from the solenoid.

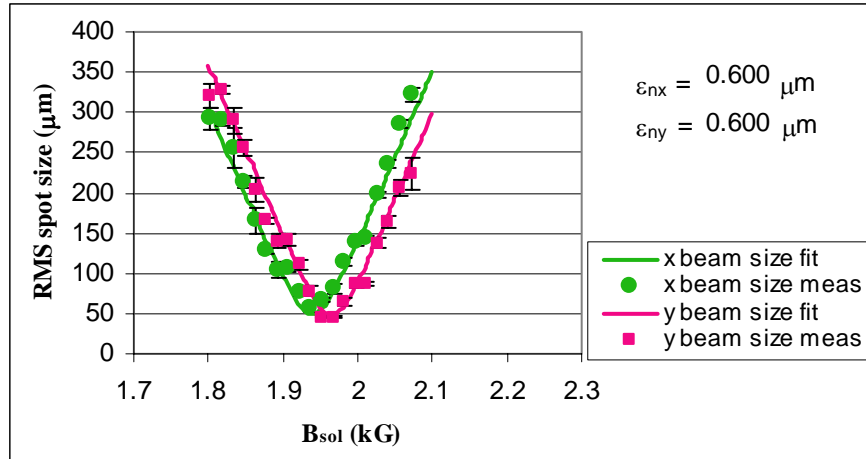


Figure 2: The x and y rms beam size vs solenoid field with the solenoid polarity identical to the left image in Figure 1.

c. Two sets of pancake coils

At the same time as the magnetic measurements were conducted, a second set of pancake coils were installed in the old magnet. The original coils did not meet the specification for having a 180° crossover between windings. The crossover was closer to 140° due to an error on the original pancake coil drawing delivered to the manufacturer. Several calculations indicated the longitudinal currents in the crossover could be responsible for the observed quadrupole field and thus the second set of coils with exactly 180 degree crossover were ordered and installed. Both sets of coils were manufactured by Stangenes Industries in Palo Alto. After the magnetic measurements were completed (described in the next section) it was determined that the second set of coils performed nearly identically with the original set.

III. PROTOTYPE SOLENOID DESCRIPTION

a. Physical Description

A picture of the prototype solenoid is shown in figure 3. It is copied from a BNL design. The solenoid is comprised of 8 pancake coils separated by 7 steel flux straighteners. The flux is returned via octagonal mirror plates at the solenoid ends and four flux returns connected between the two mirror plates. The mirror plates and flux return reduce the field at the cathode to approximately 20 G with the solenoid upstream edge (50% field level) 10.0 cm from the cathode. Thus no bucking coil to reduce the field at the cathode is required.

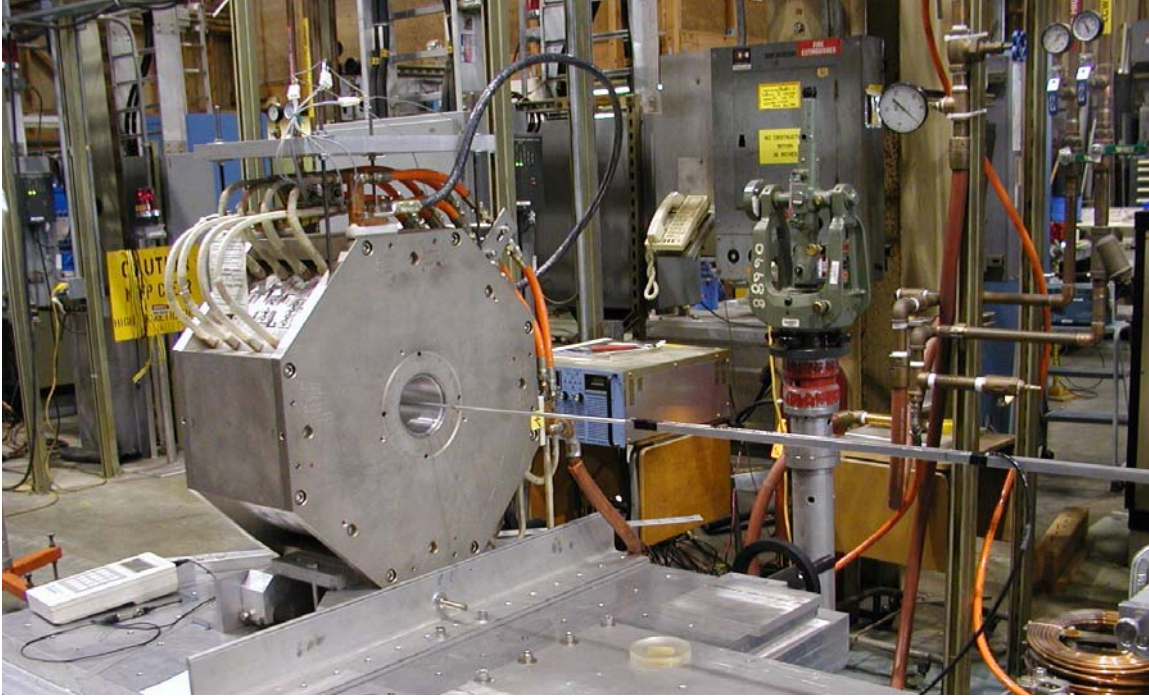


Figure 3: The GTF solenoid undergoing magnetic measurements.

A photo of an individual coil is shown in figure 4 with 29 turns. All eight pancakes are identical in the GTF solenoid. Adjacent pancake coils are rotated about the solenoid axis by 180 degrees such that the odd pancake coil leads exit at -45 degrees with respect to the horizontal axis and the even coil leads exit at 135 degrees. The conductors are 0.2893" square Cu wire with rounded corners and a 0.161" diameter hole in the center for water cooling. The conductors are wrapped with an approximately 7 mil thick insulator prior to winding to prevent shorted windings. The conductor in each pancake spirals from the outside in. At the ID the winding crosses to the second layer and then spirals out. The crossover between layers was specified to occur over 180 degrees in an attempt to minimize the transverse fields that arise from the longitudinal current component. With adjacent pancakes rotated by 180 degrees the dipole term is theoretically cancelled at the mid-plane between adjacent pancakes. The wound coil is then potted inside an Aluminum ring around the OD. The pancakes are mounted in the solenoid with rods through the Al ring which are tied to the mirror plates.

The flux straighteners serve to space the coils and guide the magnetic flux along the geometric axis of the solenoid. The location of the flux straighteners defines the magnetic axis and not the position of the coils inside the pancake. This simplifies the manufacturing of the pancake as no precise positioning of the coil within the potted pancake is required. The flux straighteners are machined out of 1006 Steel and are mounted over an Al tube.

The mirror plates and flux returns are also machined from 1006 steel and are plated with a thin coat of Ni to prevent rusting and corrosion. The mirror plates are octagonal shaped with a distance of 17.391" across the flats. The mirror plates mount on the Al tube with the 4 flux returns mounting between the mirror plates at the OD. The total length of the solenoid is 22.5 cm. The four flux returns are positioned at the top, bottom, left and right sides of the octagonal mirror plates. Holes for tooling balls are machined in

the top of the mirror plates for alignment fiducials. The entire solenoid except the pancakes and ceramic spacers between the flux straighteners were machined at SLAC. The ceramic spacers were manufactured by Wesgo Duramic in New Jersey. Dimensions of the GTF and LCLS solenoid are listed in section V.

The maximum operating current in the prototype solenoid is 275 A and the total magnet impedance is approximately 0.1Ω . The magnet is water cooled with 3.6 GPM of water flow and a 74 PSI pressure drop across the solenoid. The pancakes are wired in series electrically using a single power supply and the water circuit is in parallel.



Figure 4: The two layer pancake coil prior to potting.

b. Magnetic Measurements

The solenoid underwent extensive magnetic measurement at the SLAC metrology department. The measurements included hall probe measurements of the on axis solenoid field vs longitudinal position at various currents. Measurements were also made 10 mm off axis and the results of these measurements are plotted in figure 5. All fields scale nearly linearly with current. The field 10 mm off axis has a maximum error of approximately 2% which is concentrated near the mirror plates. The off axis field displays an asymmetry between the upstream and downstream mirror plates which is most likely due to an angular alignment error of the magnetic probe. The identical measurement with the initial pancakes installed showed no asymmetry.

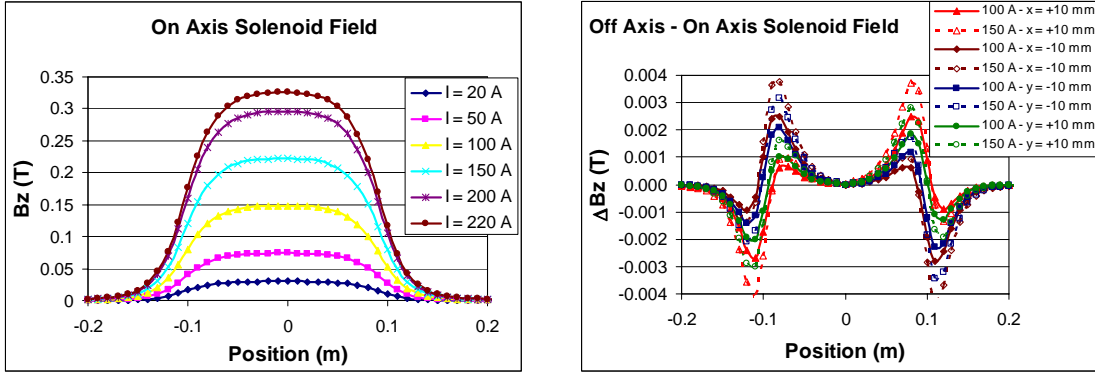


Figure 5: The on axis field vs longitudinal position is plotted on the left for six different currents. The difference of the field 10 mm off axis and the field on axis is plotted on the right for two different currents.

The peak solenoid field vs current for multiple current cycles was also measured and the results plotted in figure 6. The solenoid exhibits very little hysteresis as the difference between the fits of the rising current vs falling current is less than 0.2% at 100 A. The effective length vs current is also plotted in figure 6 showing it is nearly independent of current. The effective length is computed from the data shown in Figure 5 as the ratio of the integral of the field and the peak field. The average effective length from the five highest currents is 19.49 ± 0.03 cm.

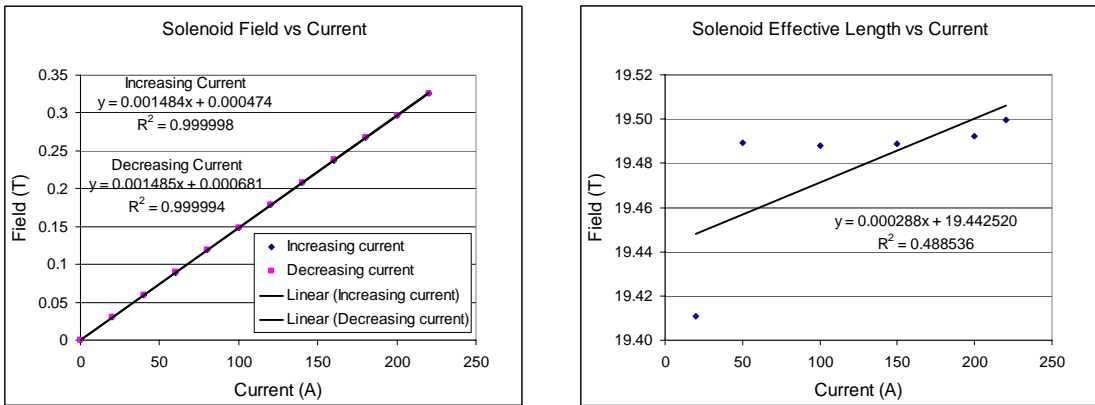


Figure 6: The plot on the left is the peak solenoid field vs excitation current and on the right is the effective length vs current.

The transverse fields were also measured as a function of position using a 3.2 cm radius short rotating coil. The fields at two currents are plotted in figure 7 showing the total transverse field is a few percent of the solenoid field at the mirror plates and $< 1\%$ of the solenoid field inside the solenoid. An ideal solenoid should have zero transverse field on axis. The measured field could be due to an alignment error but an offset or angle should produce a constant transverse field. Thus additional measurements were made of the transverse field looking at the multi-pole components of the field. Most of these measurements were made with a long rotating coil that integrated the fields through the full length of the solenoid.

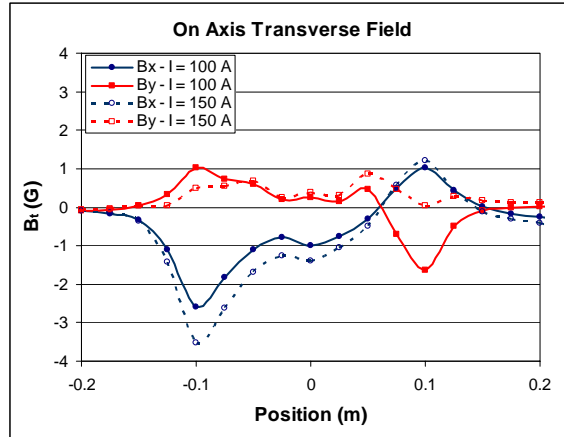


Figure 7: Transverse field on axis versus position.

Additional magnetic measurements were conducted with a magnetic probe on a rotating coil at a 2.70 cm radius connected to a spectrum analyzer to measure the multipole modes present in the solenoid. The first 4 multipole modes measured with a long probe that integrates the magnetic field over the entire length of the solenoid are shown in figure 8. The focal length of the quadrupole assuming 130 A solenoid current and a 5.5 MeV beam is approximately 30 m. The magnetic measurement probe was carefully aligned with respect to the solenoid and the power supply leads entered and exited from the solenoid radially to eliminate the current dependent component of the dipole. The remaining dipole field is contributed from the earth's magnetic field. The quadrupole term is a linear function of current with nearly zero intercept indicating the field is clearly due to the current in the pancakes with very little hysteresis. The measured phase is defined as the position of the first south pole with respect to the starting position of the probe. Neither the amplitude or phase of the quadrupole, sextupole or octopole terms changed significantly from measurement to measurement.

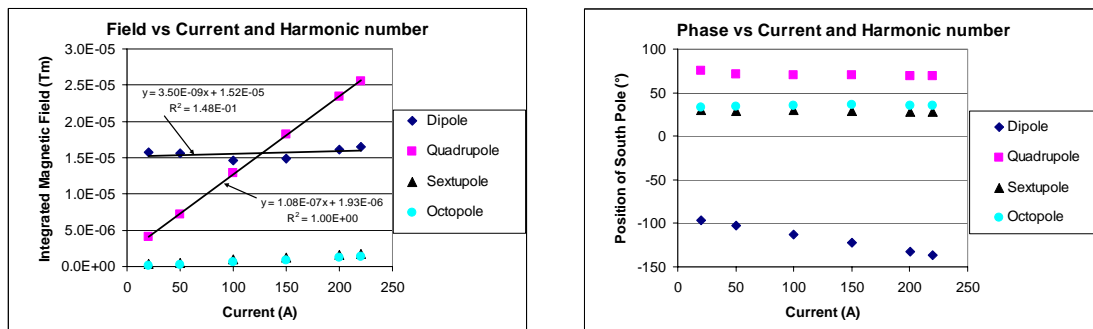


Figure 8: The amplitude and phase of the dipole, quadrupole, sextupole and octopole terms as a function of solenoid current.

The focal length is nearly identical with the original and final sets of pancakes. Since the geometry of the coil crossover was not responsible for the quadrupole term additional measurements were conducted to understand the source of the quadrupole term. Therefore, measurements with only two pancake coils and no additional steel were conducted. The results are listed in table 2 and should be compared to the slope and

intercept shown in figure 8 for the full solenoid with 8 pancakes. To first order the quadrupole terms from each pancake should be identical and thus should add with 0° rotation about the longitudinal axis and subtract with 90° rotation. Thus it was anticipated that the quadrupole term from two pancakes with 0° rotation should be approximately 25% of the quadrupole term measured in the GTF solenoid but instead it is closer to 10%. Second, the quadrupole term should be minimized when the coils were rotated by 90° but in fact it was maximized. Finally the 0° and 180° results should be nearly identical but the measurements differ by 40%. The best explanation for the difference between the expected and measured results is the longitudinal dependence of the quadrupole field. Each pancake is translated with respect to each other and the total measured field is the vector addition of each quadrupole field. The intercept is identical for all cases including the full solenoid which seems to indicate the intercept is the result of a stray field or measurement error. Other measurements not reported here had varying intercepts including negative values. A 65 G permanent magnet was placed on the outside of the solenoid housing and a measurement made with 0 A solenoid current. The measured quadrupole field was nearly two orders of magnitude larger than the intercept listed in table 2. Thus a mere 1 G external field could produce the measured intercept.

Table 2: The slope and intercept of the quadrupole term for two pancakes side by side with the second coil rotated about the longitudinal axis with respect to the first coil.

$\theta_2 - \theta_1$	Slope	Intercept
0°	$1.4 \cdot 10^{-8} \text{ Tm/A}$	$1.9 \cdot 10^{-6} \text{ Tm}$
90°	$2.0 \cdot 10^{-8} \text{ Tm/A}$	$1.9 \cdot 10^{-6} \text{ Tm}$
180°	$1.0 \cdot 10^{-8} \text{ Tm/A}$	$1.9 \cdot 10^{-6} \text{ Tm}$

Thus the longitudinal dependence of the solenoid dipole, quadrupole and sextupole fields were measured with a short rotating coil probe at radius at 2.86 cm and the result is plotted in figure 9. As the plot shows the dipole field is present throughout the length of the solenoid with a nearly constant south pole position. This could be explained with a small angular misalignment of the probe to the solenoid. However, the quadrupole term is dominantly present around the two mirror plates. The south pole is at roughly 0° on the upstream mirror plate and 90° at the downstream mirror plate. The sextupole term is very small as expected from the previous measurements.

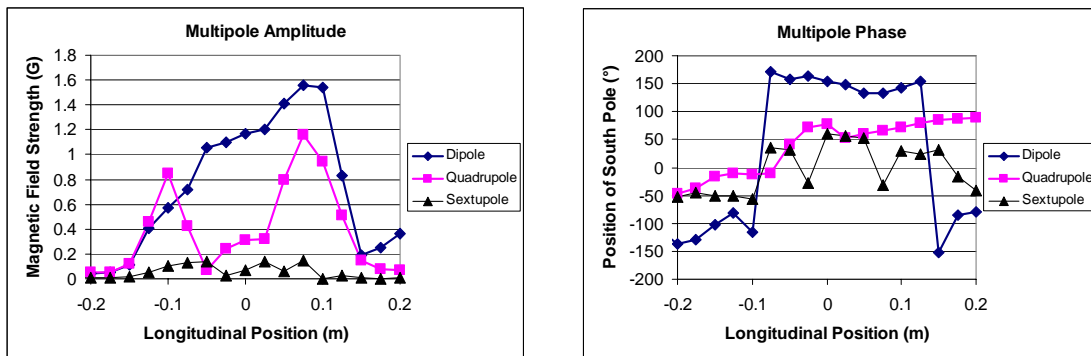


Figure 9: The amplitude and phase of the dipole, quadrupole, and sextupole terms as a function of longitudinal position at a current of 100 A.

The measurements were then numerically integrated and the results for three excitation currents are plotted in figure 10. Figure 10 should be compared with figure 8. The difference in the dipole terms is most likely due to an angular misalignment as described above. The quadrupole term from the numerical integration is about 70% of the long rotating coil measurement while the sextupole term is 90%. The discrepancy may be due to the different radii of the two probes used in the measurements.

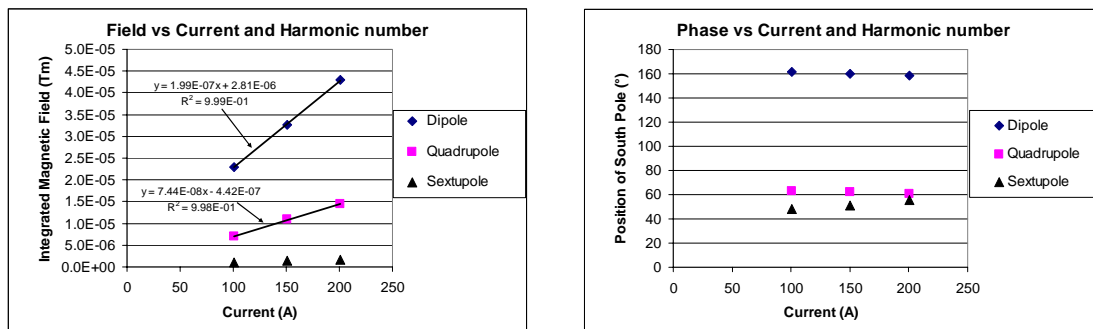


Figure 10: The amplitude and phase of the dipole, quadrupole, and sextupole terms as a function of solenoid current. The results are numerically integrated from the data plotted in figure 9.

At this time there is no proven explanation of the source of the quadrupole term. It was considered that the quadrupole is due to the four flux returns. However, simulations by Carr [7] showed that the octupole term would dominate over the quadrupole term. Since the measured data clearly show the octupole term much weaker than the quadrupole term, the effect must be due to another source. The most likely source is the longitudinal current in the pancake crossover layer. In the interior of the solenoid the fields from adjacent pancakes may cancel while at the ends there is no additional pancake source to cancel the field. The quadrupole field at the solenoid ends may be amplified by the presence of the steel mirror plates. However, since the quadrupole source was not clear, the effort shifted to methods to eliminate or cancel the quadrupole term.

IV. CORRECTION SCHEMES

The first attempt to eliminate the transverse fields was to wind a permeable material in a helical fashion along the length of the solenoid inner bore as suggested by Carr [7]. The idea was to shunt undesired flux through the permeable material. The solenoid field should not be affected since the solenoid field is orthogonal to the material. Ideally, the only effect should be the reduction of the undesirable transverse fields.

The inner bore of the solenoid is 2.90" and the OD of the SPEAR 3 rotating coil used for quadrupole magnetic measurements is 2.53". The OD of the vacuum flange inserted inside the solenoid is 2.73". Thus an acrylic tube with 2.75" ID and 3.00" OD was obtained and the OD turned down to 2.85". The tube was wound over the central 8" with a permeable wire of diameter 0.005". The tube was then inserted inside the solenoid and

multi-pole magnetic measurements performed. Unfortunately the shield had no measurable effect on the quadrupole field.

The second attempt concentrated on canceling the quadrupole field instead of eliminating the field. Thus a 4 wire quadrupole was constructed with 22 gage wires at 3.6 cm radius on the OD of an acrylic tube. The single wire runs the full length of the solenoid then rotates 90° at a constant radius and returns. This is repeated two more times to produce a total of four longitudinal wires with identical current and adjacent wires have opposite polarity. A picture of the corrector used in the experiment is shown in figure 11. The on axis dipole and quadrupole fields generated from a 4 wire corrector are given in equations 2 and 3. I_n is the current and x_n, y_n are the coordinates of the n^{th} wire. With the 4 wire corrector quadrupole setup described above and with the wires positioned symmetrically on the x and y axis for the, both dipole terms and the skew quadrupole term cancels with the regular quadrupole the only remaining field. It is expected that approximately 6 A in the corrector is required to cancel the solenoid quadrupole with 150 A excitation current.

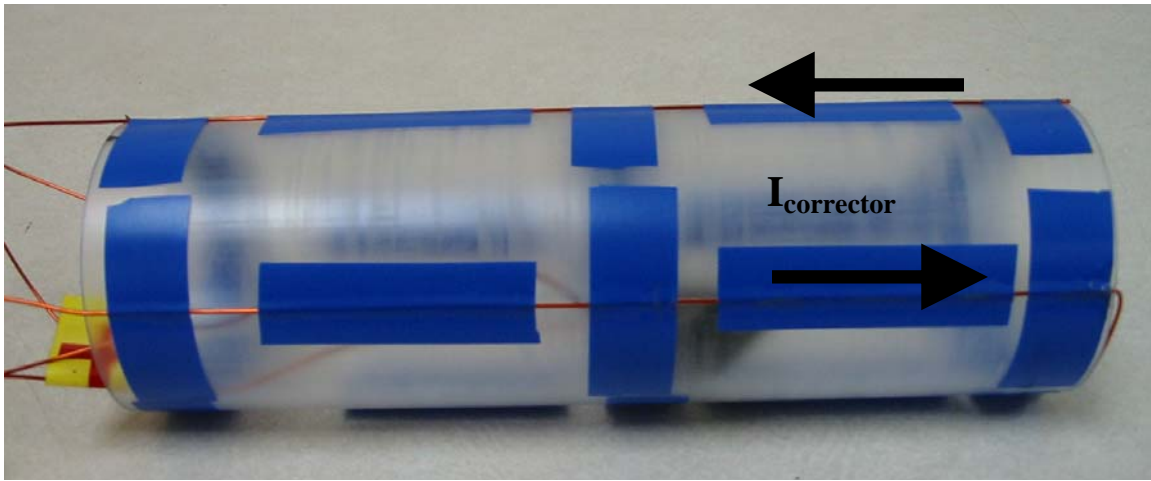


Figure 11: The 4 wire quadrupole corrector attached to a 2.85” OD acrylic tube is shown. The single wire starts and ends on the left. Adjacent wires have identical current but opposite polarity forming a quadrupole in the center of the tube.

$$M_x \equiv B_x \Big|_{x,y=0} = \frac{\mu_0}{2\pi} \sum_{n=1}^N \frac{I_n y_n}{x_n^2 + y_n^2} \quad \text{dipole} \quad 2$$

$$M_y \equiv B_y \Big|_{x,y=0} = \frac{\mu_0}{2\pi} \sum_{n=1}^N \frac{-I_n x_n}{x_n^2 + y_n^2} \quad \text{dipole}$$

$$g \equiv \frac{\partial B_x}{\partial y} \Big|_{x,y=0} = \frac{\partial B_y}{\partial x} \Big|_{x,y=0} = \frac{\mu_0}{2\pi} \sum_{n=1}^N \frac{I_n (y_n^2 - x_n^2)}{(y_n^2 + x_n^2)^2} \quad \text{quadrupole} \quad 3$$

$$\hat{g} \equiv -\frac{\partial B_x}{\partial x} \Big|_{x,y=0} = \frac{\partial B_y}{\partial y} \Big|_{x,y=0} = \frac{2\mu_0}{2\pi} \sum_{n=1}^N \frac{-I_n x_n y_n}{(y_n^2 + x_n^2)^2} \quad \text{skew quadrupole}$$

The corrector was placed inside the solenoid and the results of the magnetic measurements are plotted in figure 12. The measurement on the left was performed with

the solenoid current at 0 A and the measurement on the right is with the corrector current at 1.8% of the solenoid current. The corrector has been rotated to nearly the optimum angle in an attempt to cancel the intrinsic solenoid quadrupole. The net result is that the corrector has reduced the total solenoid quadrupole by nearly an order of magnitude.

The corrector current necessary to nearly cancel the solenoid quadrupole was lower than expected. This is likely due to the large diameter of the magnetic probe used in the experiment. The probe radius of 2.7 cm is close to the 3.6 cm corrector wire radius. This will increase the measured corrector field compared to the field on axis. However, the electron beam will interact with the on axis field and therefore when attempting to eliminate the effect on the electron beam it is expected that the corrector current will need to be increased to roughly 6 A.

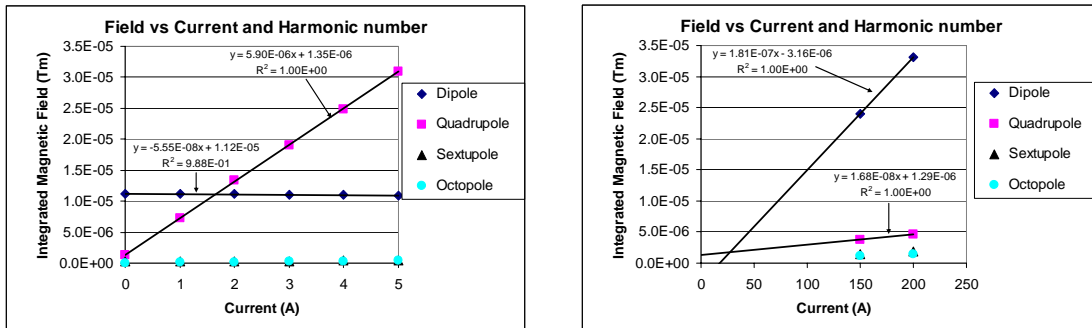


Figure 12: The multi-pole amplitudes as a function of corrector current with the solenoid current at 0 A is plotted on the left. On the right is the multi-pole amplitude as a function of solenoid current with the corrector at 2.7 A and 3.6 A for the solenoid current at 150 A and 200 A respectively.

Thus it is clear that a four wire corrector can be used to nearly eliminate the total integrated quadrupole term. However, that does not mean it will eliminate the quadrupole effect on the electron beam. Since the beam rotates as it travels through the solenoid, the focusing in the transverse planes is coupled and can not be exactly cancelled unless the quadrupole field is cancelled at each point in space. However designing a quadrupole that has the same spatial profile as the solenoid quadrupole term is impractical.

Nonetheless a simple quadrupole corrector can reduce the effect to insignificant levels. As can be seen in figure 9, the quadrupole phase at the downstream mirror plate is rotated roughly 90° from the upstream mirror plate. At the LCLS beam energy of 6 MeV, the solenoid will rotate the beam approximately 75° as it travels through the solenoid. Thus the beam experiences similarly oriented quadrupoles at both mirror plates and the solenoid quadrupole can be largely cancelled with an externally applied quadrupole such as the 4 wire quadrupole. Therefore the LCLS solenoid design included a 4 wire quadrupole. In reality the design includes 2 independent 4 wire quadrupoles rotated at 45° to allow for an electrically adjustable quadrupole orientation. This eliminates the alignment problem setting the corrector angle with respect to the solenoid. Instead the problem is shifted to injector commissioning where the proper setting of the two 4 wire quadrupoles must be determined.

V. LCLS GUN SOLENOID

The LCLS solenoid is basically a copy of the GTF solenoid with the quadrupole and dipole correctors added. A completely different design with helical windings was considered but not implemented because of the constant longitudinal current component that produces a transverse field and the cooling problem with a long coil. Thus based on the measurements shown above the LCLS gun solenoid specifications listed in table 1 were generated.

The two step design goal of the LCLS solenoid was to first minimize the multi-pole contribution from each pancake and then minimize the vector sum of the individual fields. This means the beam should exit the solenoid on axis and parallel to the axis [7]. In other words the first and second integral of the dipole field should be zero. In addition the first and second quadrupole field integrals should be zero such that the beam size and angle does not change due to the quadrupole field.

In order to minimize the multi-pole fields from a single pancake the optimum crossover angle must be determined. The ideal crossover angle would minimize all the multi-pole fields. Since two adjacent dipoles rotated by 180° degrees with respect to each other cancel, the dipole term from a 360° crossover is to first order zero since each dipole field from a transverse segment of current cancels an identical field from a current segment rotated by 180° . Likewise the quadrupole term is minimized for a crossover angle that is a multiple of 180° . The n_{th} order multi-pole field cancels if the crossover is a multiple of $720^\circ/n$. Thus for a thin 2 layer pancake and ignoring the effect of nearby permeable material, the ideal crossover angle is 360° . However, a 360° crossover is impractical since the first and second layer interfere at the crossover and the two layer pancake must be at least three conductor widths wide to achieve 360° . Thus a 180° crossover was chosen so that the pancake width could be minimized. The 180° crossover cancels all the multi-pole fields except the dipole term. Thus it is important that the pancakes are assembled in proper sequence such that adjacent pancakes cancel the dipole term.

There are two options for constructing the pancakes with 180° crossover [8]. In one type the wire spirals in clockwise at the upstream end and then spirals out clockwise at the downstream end. The second type is the mirror image about the magnetic axis of the first type such that the solenoid field from the two pancakes interferes constructively and the multi-pole fields destructively interfere. Thus the mirror image coil spirals in clockwise from the downstream end and then spirals out clockwise at the upstream end. The two types of coils are shown in figure 13 along with the same coils rotated about the magnetic axis by 180° . All the multi-pole fields in the mirror image coil have opposite polarity compared to the regular coil. Thus a regular and mirror image coil can be used as an adjacent pair to cancel the dipole term. Alternatively, the second of identical, adjacent pancakes can be rotated 180° about the magnetic axis in order to cancel the dipole term. All pancakes have 29 turns and identical electrical properties. The only difference is in the multi-pole field polarities.

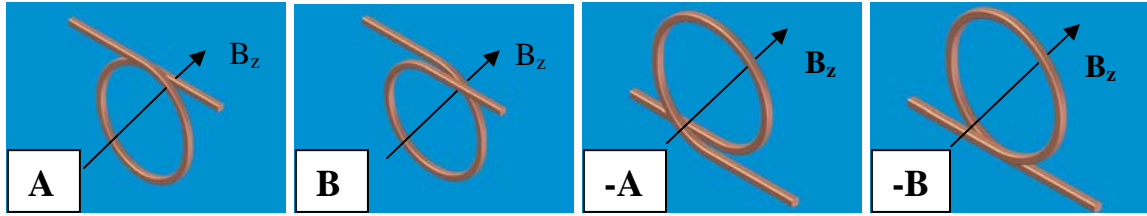


Figure 13: A regular coil (type A), mirror image coil (type B), regular coil rotated 180° (type -A) and a mirror image coil rotated 180° (type -B) shown from left to right.

The four different pancake types produce different polarity quadrupole and dipole terms. Clearly the B pancake produces multi-pole fields with opposite polarity to the A pancakes. The -A pancake produces multi-pole fields with the same polarity to the A pancake except for the dipole term. The results for the quadrupole and dipole terms are summarized in table 3.

Table 3: Dipole and quadrupole polarities of the 4 pancake styles.

Pancake Type	A	-A	B	-B
Dipole polarity	+	-	-	+
Quadrupole polarity	+	+	-	-

The six possible methods for assembling 8 pancakes that have zero first and second integrals of the dipole and quadrupole term and also have every adjacent pancake pair cancel the dipole term are shown in table 4. With all options the beam will exit parallel to and on axis and with no change in beam size or angle due to the quadrupole term. However, option 4 (highlighted in red) minimizes the expected deviation of the beam off axis and the focusing kick. In other words the second integral of both the dipole and quadrupole field undergoes one full period of sinusoidal variation through the length of the solenoid. Since the desire is to minimize the steering and focusing effect on the beam, option 4 was chosen for the LCLS gun solenoid design.

Table 4: Possible pancake configurations to cancel the first and second integrals of the multi-pole fields.

Pancake	#1	#2	#3	#4	#5	#6	#7	#8
Option 1	A	-A	B	-B	B	-B	A	-A
Option 2	A	-A	B	-B	-B	B	-A	A
Option 3	A	B	B	A	A	B	B	A
Option 4	A	B	B	A	B	A	A	B
Option 5	A	B	-A	-B	-B	-A	B	A
Option 6	A	B	-A	-B	B	A	-B	-A

Option 4 is a different sequence than used in the prototype solenoid. The prototype solenoid was constructed from alternating A and -A pancakes. Thus the prototype solenoid had adjacent pancake leads exit on opposite sides of the solenoid. The LCLS solenoid will have all eight pancake leads exit on one side. This was considered an advantage as it simplified the electrical connections and the water manifold design.

In order to cancel any remaining quadrupole field, regular and skew quadrupole correctors were added each capable of producing a 20 m focal length as discussed in the previous section. In addition two orthogonal dipoles capable of deflecting the beam by 10 mrad were added to the design to compensate for solenoid misalignments. This orthogonal corrector design allows the dipole and quadrupole to be electrically rotated to any desired orientation.

The prototype solenoid had to be modified to allow the insertion of the 4 wire correctors. To conserve space the 4 wire quadrupoles were incorporated into the inner bore tube design. Two sets of slots were milled along the length of the tube and 16 gage magnet wires are glued into the slots. One set of four wires is at 3.268" diameter and the second set is at 3.393" radius. Since the ID of the tube could not be reduced due to the beam-pipe flange OD, the tube OD was increased to house the corrector. Originally it was intended that the 4 wire corrector could be powered by two separate power supplies so that a dipole field could also be generated and both orthogonal dipole and quadrupole correctors would be implemented with a total of 8 wires. However, from equation 2 it is clear that in order to steer the beam 10 mrad with the dipole it would require approximately 100 A of corrector current. From equation 3 the quadrupoles requires less than 12 A to produce a 20 m focal length. Since 100 A exceeds the current capability of the 16 gage wire, a separate pair of dipoles were added that mount on the 1.5" OD beam-pipe inside the solenoid. The dipole and quadrupole correctors are shown in figure 14. The dipole uses 20 turns of 16 gage magnet wire. These dipole correctors only require 10 A of current to steer the beam 10 mrad.

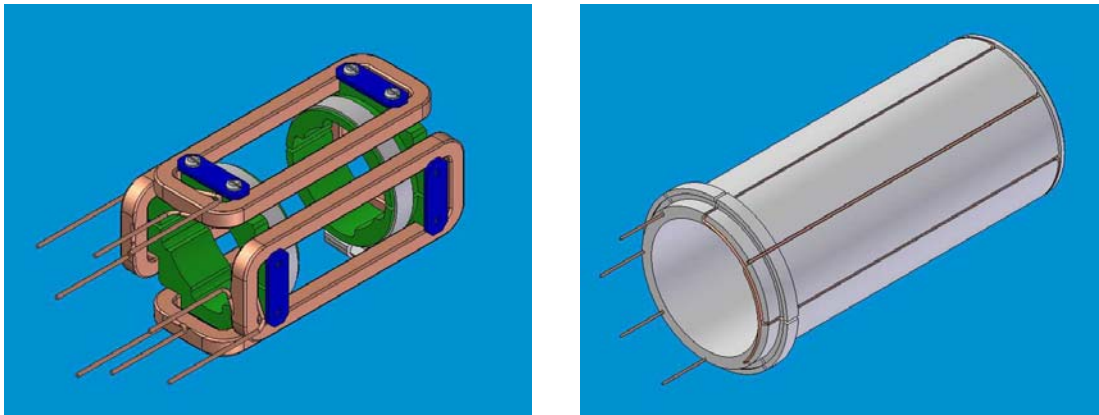


Figure 14: A 3D image of the LCLS gun solenoid horizontal and vertical dipoles (left) and the two 4 wire quadrupoles (right) correctors.

A complete list of the solenoid dimensions is shown in table 5 along with a comparison of the dimensions in the prototype solenoid. The coil dimensions are unchanged. The ID of the flux straighteners and mirror plates were modified to allow the insertion of the 4 wire quadrupoles. One of the main dimensional changes was to the thickness of the mirror plates. PARMELA simulations indicated the need to move the rising edge of the solenoid closer to the cathode [5]. However, the prototype solenoid is adjacent to the gun and can not be translated closer to the cathode. Since the solenoid effective length is less than the physical length it was possible to thin the mirror plates without changing the magnetic field profile. Thus the mirror plate thickness was reduced

from 0.700” to 0.375”. The 8 mm difference is sufficient to move the solenoid edge to the desired position relative to the cathode and the thinner mirror plate can still accept the peak solenoid flux without saturation [7]. A 3D image of the solenoid is shown in figure 15.

Table 5: Comparison of LCLS and GTF solenoid Dimensions

Dimension	GTF	LCLS
Conductor		
Width	0.2893”	0.289”
Center Hole Diameter	0.161”	0.161”
Coil		
ID	4.724”	4.724”
OD	14.241”	14.234”
Thickness	0.639”	0.639”
Potted Pancake		
ID	4.575”	4.575”
OD	15.391”	15.391”
Thickness	0.760”	0.760”
Flux Straightener		
ID	3.150”	3.410”
OD	9.250”	9.250”
Thickness	0.125”	0.125”
Inner Bore Tube		
ID	2.900”	2.900”
OD	3.1485”	3.408”
Length	8.522”	8.010”
Mirror Plate		
ID	3.150”	3.410”
OD-Flat to Flat distance	17.391”	17.391”
Thickness	0.700”	0.375”
Flux Return		
Length	7.459”	7.459”
Width	7.204”	7.204”
Thickness	1.000”	1.000”
Complete Solenoid		
ID	2.900”	2.900”
OD-Flat to Flat distance	17.391”	17.391”
Length	8.859”	8.209”

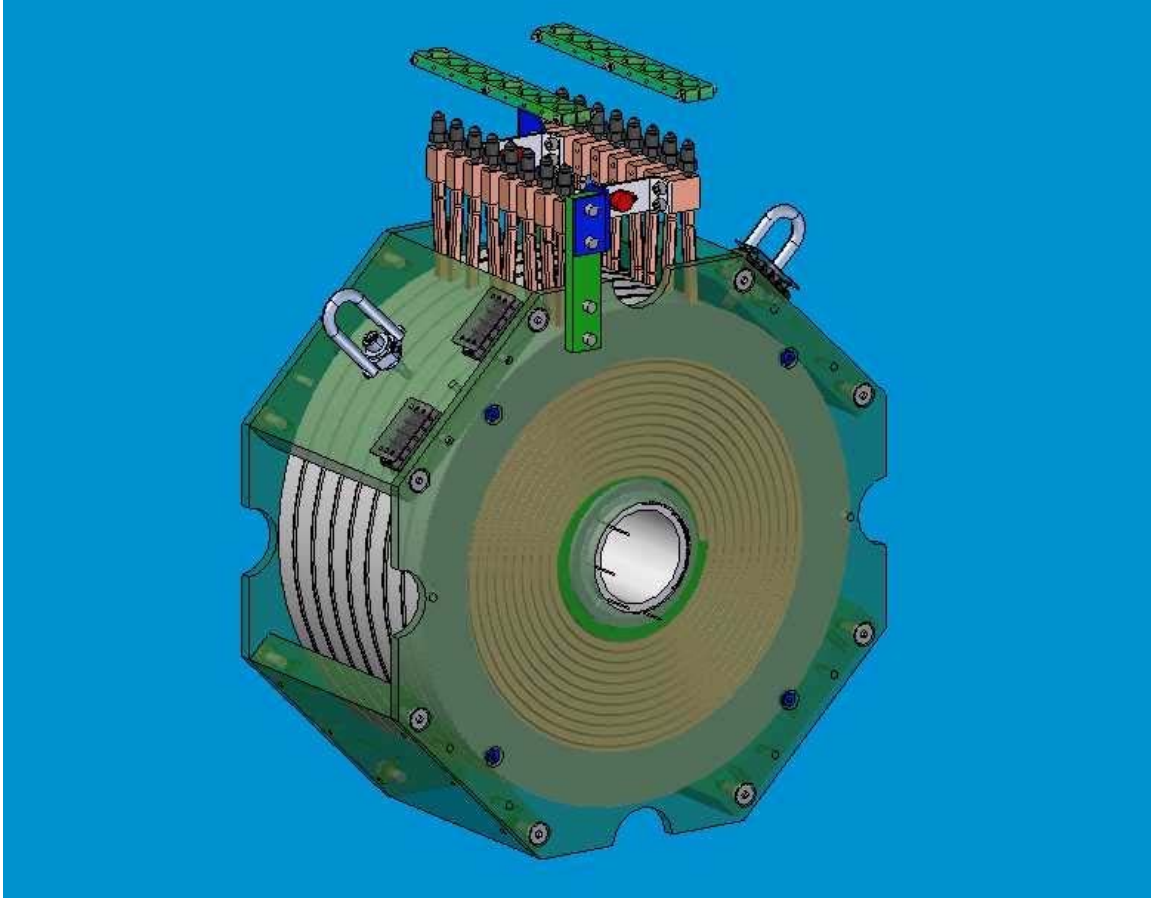


Figure 15: The mechanical drawing of the LCLS with all the suggested modifications.

VI. OTHER MODIFICATIONS

Another change to the solenoid is the careful positioning of the power supply leads. Since the power supply requires up to 275 A, the magnetic field from the leads can be undesirable. In order to keep the leads as far from the electron beam as possible the leads should enter and exit the magnet orthogonal to the magnetic axis. During magnetic measurements on the prototype solenoid, the leads often contributed to the measured dipole terms. Only with careful positioning of the leads was the dipole term completely suppressed as demonstrated in figure 8.

In addition to the changes that affect the magnetic field there were several other modifications suggested based on GTF operational experience. First, the dipole and quadrupole corrector were designed to withstand a high temperature bake. The gun along with the beam-pipe inside the solenoid will require periodic bakes up to 200° C. Thus the inner bore of the solenoid will also be required to withstand the bake. The materials and epoxy used in the corrector construction are designed to withstand 200° C. In addition, the dipole corrector was designed to allow sufficient space for a heater tape to be wound on the OD of the beam-pipe. The heater tape is intended to remain in place after the

bake. Thermocouples can be added to the solenoid ID to monitor the solenoid temperature during the bake.

Notches were added to the mirror plates to increase the clearance for the laser beam passing near the magnet for grazing incidence cathode illumination. The notches are 1” semicircles at the outer diameter of the mirror plates in between the flux returns as seen in figure 15. The notches were placed symmetrically on both mirror plates at a location of minimal flux to avoid affecting the magnetic field. Simulations were performed to confirm the notches had a negligible effect on the magnetic field [7]. The LCLS solenoid will also be rotated 45° about the solenoid axis with respect to the prototype solenoid so that the notch will align with the laser port in the gun half cell.

The final modification is the need for a bipolar power supply. A bipolar supply is preferred for magnetic standardizations and it allows for quick polarity changes without shutting off the electron beam. This will be particularly useful for beam studies during injector commissioning.

VII. SUMMARY

The LCLS gun solenoid is based on the prototype solenoid installed at the GTF for over eight years. Based on magnetic measurements, operational experience and beam tests with the GTF gun solenoid multiple modifications are suggested for the LCLS gun solenoid. The modifications include the following:

1. Adding horizontal and vertical dipole correctors inside the solenoid.
2. Adding normal and skew 4 wire quadrupole correctors inside the solenoid.
3. Modifying the solenoid dimensions to accommodate the correctors.
4. Decreasing the mirror plate thickness to allow the solenoid to move closer to the cathode.
5. Notches cut in the mirror plate around the gun cathode laser ports to allow greater optical clearance with grazing incidence cathode illumination.
6. Utilizing pancake coil mirror images to compensate the first and second integrals of the transverse fields.
7. Forcing all the pancake leads to exit on the same side to compensate the first and second integral of the transverse fields. This also simplified the water manifold since all the water connections are on one side of the solenoid.
8. Requiring the DC power supply leads to enter radially to reduce the dipole term.
9. Incorporating a bipolar power supply to allow for proper magnet standardization and quick polarity changes.
10. Increased clearance for heater tape around the vacuum pipe inside the solenoid to be used during gun bake outs.

These modifications are expected to improve the electron beam quality delivered by the injector and to make it easier for the operator to diagnose electron beam related problems at the gun exit.

Finally the design presented here is specifically for the LCLS gun solenoid although it could in principle apply to the solenoid around the first injector linac section.

However, since the solenoid field required in this solenoid is less than the gun solenoid and the beam energy is higher in the linac solenoid it is expected that the transverse field quality would be achieved with other designs as well.

VIII. ACKNOWLEDGEMENTS

I would like to acknowledge the contribution of many colleagues at the GTF including Jym Clendenin, Dave Dowell and Steve Gierman. We have all had numerous discussions regarding the desired magnetic measurements for the GTF solenoid and the effect of those measured fields on the electron beam. A special acknowledgement to Steve Gierman for all his work in trying to understand the source of the GTF electron beam asymmetry. Steve conducted numerous experiments and calculations to track down the source and I have borrowed liberally from his work.

I would like to acknowledge Cecile Limborg for providing the electron beam simulation results. Cecile and I compared the solenoid fields used in the LCLS PARMELA simulations with the measured results until we were confident we had the minimum emittance possible with a solenoid field that could be produced in the lab.

I would also like to thank Zack Wolf and his group in the SLAC metrology department that performed all the magnetic measurements. They performed numerous measurements over the course of several months and never complained with the often futile attempts to eliminate the quadrupole field.

I must also give a special acknowledgment to Mike Palrang for his hard work modifying and correcting all the solenoid mechanical drawings. This is tedious work and Mike did it all very efficiently. Mike also designed the new dipole and quadrupole correctors and supplied me with the 3D images included in this report.

Finally I wish to thank Roger Carr and Jack Tanabe for the discussions about the source and various methods for eliminating the quadrupole field measured in the GTF solenoid. Both Roger and Jack suggested many of the modifications incorporated in the LCLS solenoid design described in this report. Roger also performed several magnetic simulations to help determine the source of the quadrupole term and verify the performance of the LCLS solenoid design.

IX. REFERENCES

-
- [1] K.J. Kim, Nuclear Instruments & Methods vol A275, pp. 201-218, 1989.
 - [2] B.E. Carlsten, Nuclear Instruments & Methods vol. A285, pp. 313-319, 1989.
 - [3] M. Reiser, 'Theory and Design of Charged Particle Beams', John Wiley & Sons, 1994.
 - [4] A.S. Gilmour, 'Principles of Traveling Wave Tubes', Artech House, 1994.
 - [5] C. Limborg, SLAC, private communication, 2005.
 - [6] D.T. Palmer, "The Next Generation Photoinjector", PhD thesis, Stanford University, p. 30, 1998.

[7] R. Carr, SLAC, private communications, 2002-2004.

[8] J. Tanabe, SLAC, private communication, 2002.